

Aims and contributions

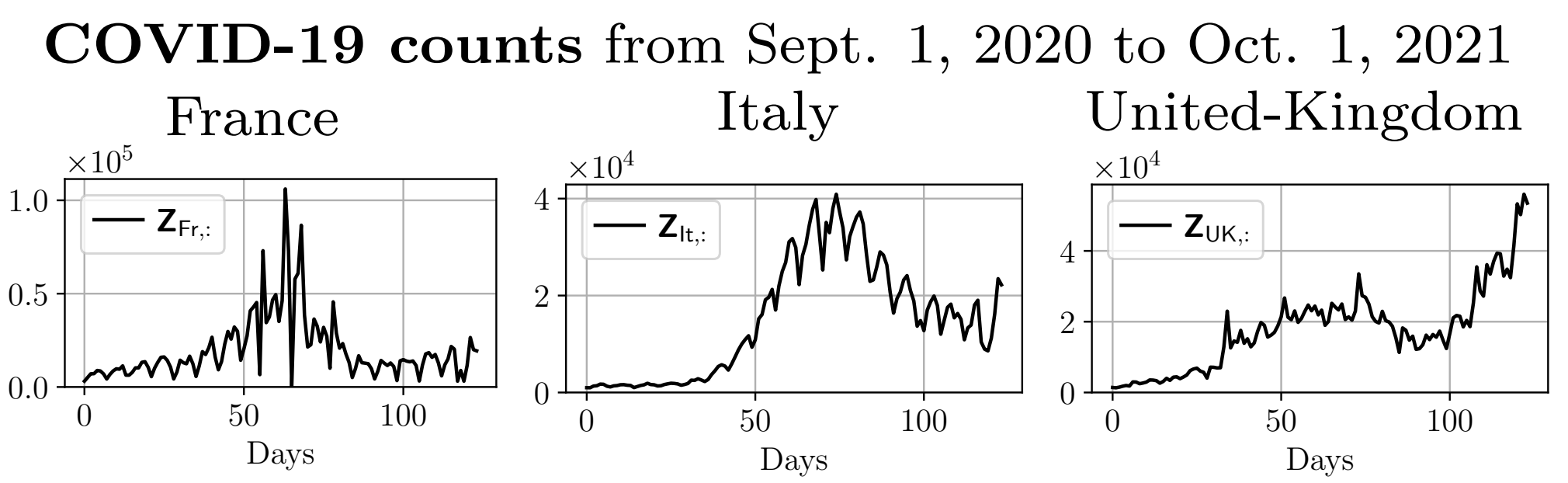
During an *epidemic outbreak*, decision makers crucially need accurate and robust tools to monitor the pathogen propagation. The *effective reproduction number* R , defined as the expected number of secondary infections stemming from one contaminated individual, quantifies the epidemic intensity. Tracking the *spatiotemporal* evolution of R during COVID-19 pandemic raised unprecedented challenges due to the *poor quality* of reported infection counts (Pascal *et al.*, 2022, *IEEE Trans. Signal Process.*).

Challenge: Infer and leverage epidemiological data's *spatial* structure to get accurate and robust R estimates.

Contributions: *joint* estimator of the reproduction number and connectivity structure

- procedure to generate *realistic* synthetic spatiotemporal epidemiological counts with *prescribed* connectivity pattern under a *scaled Poisson* model;
- spatial structure inferred via an *original* graph Laplacian estimation under Poisson *data-dependent* noise;
- *accuracy* of the joint estimator assessed through intensive numerical simulation on synthetic data, and illustration on *real* COVID-19 data.

Outcome: Data-driven algorithm to estimate *spatiotemporal reproduction numbers* from low quality counts <https://github.com/elasalle/EpiJointSpatiotempEstim>.



Source: <https://coronavirus.jhu.edu/>

Spatiotemporal model

Epidemic monitoring: *spatiotemporal* framework

- country $c \in \{1, \dots, C\}$, $C \in \mathbb{N}^*$,
- day $t \in \{1, \dots, T\}$, $T \in \mathbb{N}^*$,

reported infections: $Z_{c,t} \in \mathbb{N} \Rightarrow$ goal: infer $R_{c,t}$

Scaled Poisson model: $\{\gamma_c > 0, c = 1, \dots, C\}$

$$\forall (c, t), \frac{Z_{c,t}}{\gamma_c} | Z_{c,1}, \dots, Z_{c,t-1}; R_{c,t} \sim \mathcal{P} \left(\frac{R_{c,t} \Phi_{c,t}^Z}{\gamma_c} \right)$$

where $\Phi_{c,t}^Z = \sum_{s=1}^{\tau_\Phi} \phi(s) Z_{c,t-s}$, ϕ : serial interval

$\{Z_{c,\cdot}, c = 1, \dots, C\}$ independent random vectors

(Cori *et al.*, 2013, *Am. J. Epidemiol.*; Abry *et al.*, 2020, *PLoS One*; Pascal *et al.*, 2025, *Signal Process.*)

COVID-19: ϕ fitted by a Gamma distribution

- of mean 6.6 days,
- and standard deviation 3.5 days.

Regularized spatiotemporal estimator:

enforces a realistic, hence smooth, behavior

- in time (Cori *et al.*, 2013),
- and across *connected* countries

given a *fixed* connectivity structure (Abry *et al.*, 2020, *PLoS One*; Pascal *et al.*, 2025, *Signal Process.*)

$$\hat{\mathbf{R}}^{\text{fix-L}} = \underset{\mathbf{R} \in \mathbb{R}_+^{C \times T}}{\text{argmin}} \sum_{c=1}^C \omega_c D_{\text{KL}}(\mathbf{Z}_{c,\cdot} | \mathbf{R}_{c,\cdot} \odot \Phi_{c,\cdot}^Z) + \sum_{c=1}^C \lambda_T \|D_2 \mathbf{R}_{c,\cdot}\|_1 + \lambda_S \sum_{t=1}^T \|\mathbf{B} \mathbf{R}_{:,t}\|_2^2$$

$$D_{\text{KL}}(\mathbf{Z}_{c,\cdot} | \mathbf{R}_{c,\cdot} \odot \Phi_{c,\cdot}^Z) = \sum_{t=1}^T d_{\text{KL}}(Z_{c,t} | R_{c,t} \Phi_{c,t}^Z)$$

with ideal weights $\omega_c > 0$: $\omega_c = 1/\gamma_c$

Heuristic: $\omega_c = 1/\text{std}(\mathbf{Z}_{c,\cdot})$

$D_2 \in \mathbb{R}^{T-2 \times T}$: second-order difference operator

$\mathbf{B} \in \mathbb{R}^{E \times C}$ incidence matrix: *connectivity*

$\Rightarrow E$ edges between the C countries: $e = \{c, c'\}$

if $c < c'$, $B_{e,c} = -B_{e,c'} = \sqrt{W_{c,c'}}$: weight of e

Example: $W_{c,c'} > 0$ iff terrestrial borders $c \sim c'$

Graph Total Variation: Laplacian $\mathbf{L} = \mathbf{B}^T \mathbf{B}$

$$\text{at fixed time } t: \|\mathbf{B} \mathbf{R}_{:,t}\|_2^2 = \mathbf{R}_{:,t}^T \mathbf{L} \mathbf{R}_{:,t}$$

smoothness of $c \mapsto \mathbf{R}_{c,t}$ in the graph's topology

If $\tilde{\mathbf{B}} \in \mathbb{R}^{C \times C}$ s.t. $\tilde{\mathbf{B}}^T \tilde{\mathbf{B}} = \mathbf{L}$: *unchanged* GTV.

Algorithmic resolution: convex, *non-smooth*

$$\text{minimize } \{F(\mathbf{R}) + G(\mathbf{K}\mathbf{R}) : \mathbf{R} \in \mathbb{R}_+^{C \times T}\}$$

$$\bullet F(\mathbf{R}) = \sum_{c=1}^C \omega_c D_{\text{KL}}(\mathbf{Z}_{c,\cdot} | \mathbf{R}_{c,\cdot} \odot \Phi_{c,\cdot}^Z)$$

$$\bullet \mathbf{K}\mathbf{R} = (\mathbf{Q}_T, \mathbf{Q}_S) = \mathbf{Q}$$

$$\bullet \mathbf{Q}_T = (D_2 \mathbf{R}_{1,\cdot}, \dots, D_2 \mathbf{R}_{C,\cdot})$$

$$\bullet \mathbf{Q}_S = (\mathbf{B} \mathbf{R}_{:,1}, \dots, \mathbf{B} \mathbf{R}_{:,T})$$

$$\bullet G(\mathbf{Q}_T, \mathbf{Q}_S) = \lambda_T \|\mathbf{Q}_T\|_1 + \lambda_S \|\mathbf{Q}_S\|_2^2$$

\Rightarrow Chambolle-Pock scheme until: precision ε

or k_{max} iterations (Chambolle *et al.*, 2011, *J. Math. Imag. Vis.*; Pascal *et al.*, 2022, *IEEE Trans. Signal Process.*; Du *et al.*, 2023, *GRETSI*)

Joint estimation strategy

Regularized and sparsity-inducing objective function: $\hat{\mathbf{R}}^{\text{Joint}}, \hat{\mathbf{L}}^{\text{Joint}} \in \text{Argmin}_{\mathbf{R} \in \mathcal{R}, \mathbf{L} \in \mathcal{L}} J(\mathbf{R}, \mathbf{L})$ with

$$J(\mathbf{R}, \mathbf{L}) = \sum_{c=1}^C \omega_c D_{\text{KL}}(\mathbf{Z}_{c,\cdot} | \mathbf{R}_{c,\cdot} \odot \Phi_{c,\cdot}^Z) + \lambda_T \sum_{c=1}^C \|D_2 \mathbf{R}_{c,\cdot}\|_1 + \lambda_S \sum_{t=1}^T \mathbf{R}_{:,t}^T \mathbf{L} \mathbf{R}_{:,t} + \lambda_L \|\mathbf{L}\|_{\text{Fro}}^2; \|\mathbf{L}\|_{\text{Fro}}^2 = \sum_{c,c'} L_{c,c'}^2$$

with admissible sets $\mathcal{R} = \{\mathbf{R} \in \mathbb{R}^{C \times T}, \text{s.t. } \forall c, t \mathbf{R}_{c,t} \geq 0\}$: *non-negativity* of reproduction numbers,
 $\mathcal{L} = \{\mathbf{L} \in \mathbb{R}^{C \times C}, \text{s.t. } \text{Trace}(\mathbf{L}) = C, \forall c \neq c' L_{c,c'} = L_{c',c} \leq 0 \text{ and } \mathbf{L} \mathbf{1}_C = \mathbf{0}_C\}$:
proper Laplacian matrix with fixed total weight, excluding trivial empty graph.

J continuous, lower-bounded, coercive in \mathbf{R} and defined on a compact set \mathcal{L} for \mathbf{L} has a *minimizer*.

Minimization w.r.t. \mathbf{R} at fixed \mathbf{L} : $\tilde{\mathbf{B}} \in \mathbb{R}^{C \times C}$ s.t.

$$\tilde{\mathbf{B}}^T \tilde{\mathbf{B}} = \mathbf{L}, \hat{\mathbf{R}}^{\text{fix-L}}$$
 from Chambolle-Pock scheme

Minimization w.r.t. \mathbf{L} at fixed \mathbf{R} :

$$\hat{\mathbf{L}}^{\text{fix-R}} = \underset{\mathbf{L}}{\text{argmin}} \lambda_L \sum_{c,c'=1}^C L_{c,c'}^2 + \lambda_S \sum_{c,c'=1}^C (\mathbf{R}_{c,\cdot}^T \mathbf{R}_{c',\cdot}) L_{c,c'}$$

s.t. $\text{Trace}(\mathbf{L}) = C, L_{c,c'} = L_{c',c} \leq 0, \forall c \neq c', \mathbf{L} \mathbf{1}_C = \mathbf{0}_C$.

- non-negative, continuous, coercive, strictly convex

\Rightarrow *unique minimizer*

- quadratic program, linear constraints: *interior point*

CVXOPT: Andersen *et al.*, 2013, *cvx.org*

Alternating optimization on \mathbf{R}, \mathbf{L} :

Input: $\mathbf{Z} \in \mathbb{R}^T, (\lambda_T, \lambda_S, \lambda_L) \in \mathbb{R}_+^3, n_{\text{max}} \in \mathbb{N}^*, \mathbf{R}^{(0)}, \mathbf{L}^{(0)}, \mathbf{M}^{(0)} \leftarrow \text{minimize}_{\mathbf{L}}(\mathbf{R}^{(0)}, \lambda_S, \lambda_L)$

$\tilde{\mathbf{B}}^{(0)} \leftarrow \text{Cholesky}(\mathbf{L}^{(0)})$; define \mathbf{K} using $\tilde{\mathbf{B}}^{(0)}$

$\mathbf{Q}^{(0)} \leftarrow \mathbf{K} \mathbf{R}^{(0)}$

for $n = 0$ to $n_{\text{max}} - 1$ do

$\mathbf{R}^{(n+1)}, \mathbf{Q}^{(n+1)} = \text{min}_{\mathbf{R}}(\mathbf{Z}, \lambda_T, \lambda_S, \tilde{\mathbf{B}}^{(n)}, \mathbf{R}^{(n)}, \mathbf{Q}^{(n)})$

$\mathbf{L}^{(n+1)}, \mathbf{M}^{(n+1)} = \text{min}_{\mathbf{L}}(\mathbf{R}^{(n+1)}, \lambda_S, \lambda_L, \mathbf{L}^{(n)}, \mathbf{M}^{(n)})$

$\tilde{\mathbf{B}}^{(n+1)} = \text{Cholesky}(\mathbf{L}^{(n+1)})$

end for

Output: number $\mathbf{R}^{(n_{\text{max}})}, \mathbf{L}^{(n_{\text{max}})}$

Numerical experiments

Synthetic multivariate scaled Poisson counts: strictly respect a *prescribed* spatial structure \mathbf{L}

Proposed generation: C abstract countries partitioned into I clusters $\mathcal{C}_1, \dots, \mathcal{C}_I$, e.g., $C = 9, I = 3$;

- for each cluster \mathcal{C}_i , one realistic synthetic COVID-19 reproduction number $\mathbf{R}_{i,\cdot}^\dagger \in \mathbb{R}_+^T$, (Du *et al.*, 2023, *GRETSI*; Du *et al.*, 2024, *EUSIPCO*)
- to enforce spatial structure: in all countries of \mathcal{C}_i *ground truth* $\forall c \in \mathcal{C}_i, \mathbf{R}_{c,\cdot}^* = \mathbf{R}_{i,\cdot}^\dagger$,
- initial counts $\mathbf{Z}_{:,0}$ fixed, and scale parameters $\gamma_c = 0.01 \times Z_{c,0}^0$ allow variability *inside* clusters,

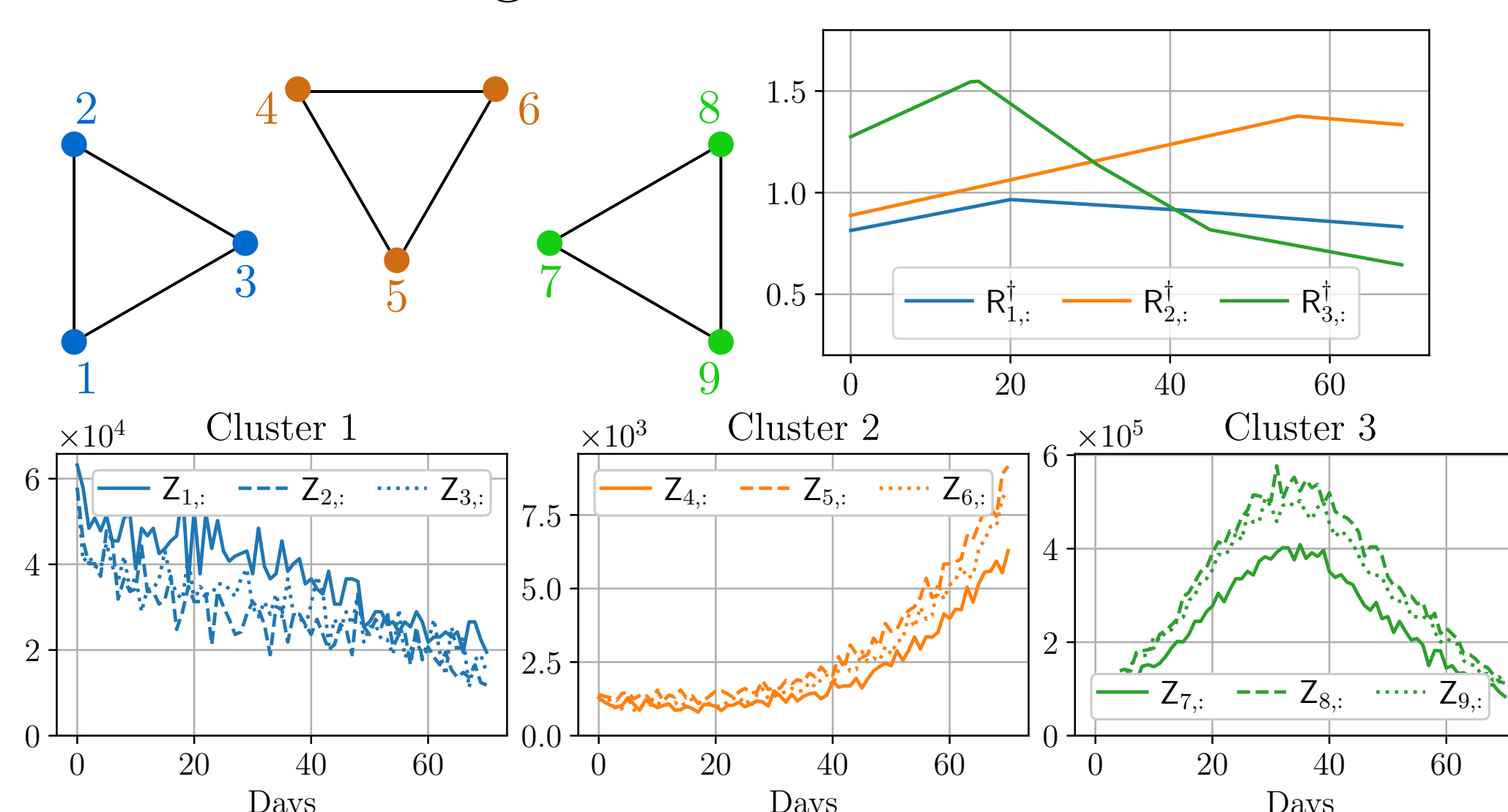
\Rightarrow synthesize scaled Poisson spatiotemporal counts $\mathbf{Z}_{c,\cdot}$ with ground truth $\mathbf{R}_{c,\cdot}^*$ independently on c .

Experimental protocol: mean Relative Squared Error $\text{mRSE}(\mathbf{R}) = \frac{1}{CT} \sum_{c=1}^C \sum_{t=1}^T \left(\frac{\hat{R}_{c,t} - R_{c,t}^*}{R_{c,t}^*} \right)^2$

- naive Maximum Likelihood estimator ML of scaled Poisson model,
- state-of-the-art epidemiological estimator EpiEstim, (Cori *et al.*, 2013, *Am. J. Epidemiol.*)
- fix-L with: an empty graph \mathbf{L}_\emptyset , *blurred* version \mathbf{L}_b of the true graph, and the true graph \mathbf{L}^* ,

Regularization parameters: optimized through *grid search*.

Performance: average and 95% Gaussian confidence intervals of mRSE over 20 *realizations*.

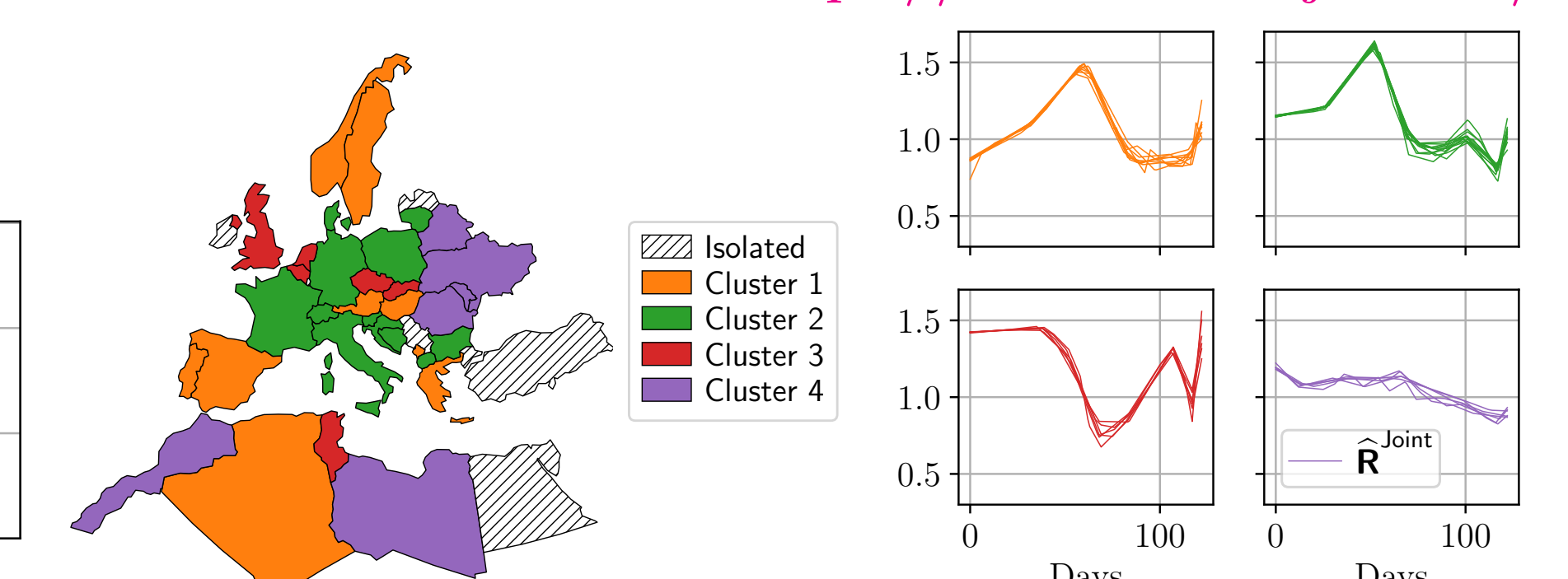


ML	EpiEstim	fix-L _∅	fix-L _b	fix-L*	Joint (ours)
113.2(±4.5)	27.7(±1.2)	9.0(±1.1)	5.4(±0.6)	2.6(±0.4)	2.7(±0.4)

$$\|\hat{\mathbf{L}}^{\text{Joint}} - \mathbf{L}^*\|_{\text{Fro}}^2 / \|\mathbf{L}^*\|_{\text{Fro}}^2 = 2.3(\pm 1.0) \times 10^{-13}$$

Real COVID-19 counts: public data from Johns Hopkins University repository

<https://coronavirus.jhu.edu/>



- 39 countries in Europe and Africa
- from Sept. 1, 2020 to Oct. 1, 2021
- manual fine-tuning of hyperparameters

Conclusions & perspectives

- joint estimator of reproduction numbers and spatial connectivity structure proposed
- numerical experiments assessing accuracy of reproduction number and spatial structure estimates
- ▶ future exploration of its robustness to changes in monitored territories and/or phase of the pandemic